Effect of Ball Milling on the Electrochemical Properties of $La_{0.7}(Mg_{0.25}Ti_{0.05})(Ni_{0.85}Co_{0.15})_{3.5}$ Hydrogen Storage Alloy

Shujun Qiu[1,2], Xingyu Ma[1], Errui Wang[1], Jianling Huang[1], Hailiang Chu[1,2,*], Yongjin Zou[1,2], Cuili Xiang[1,2], Fen Xu[1,2] and Lixian Sun[1,2]

[1]*Guangxi Key Laboratory of Information Materials, School of Materials Science and Engineering, Guilin University of Electronic Technology, Guilin 541004, China*
[2]*Guangxi Collaborative Innovation Center of Structure and Property for New Energy and Materials, Guilin 541004, China*

Abstract The influence of ball milling on the structure and the electrochemical properties of $La_{0.7}(Mg_{0.25}Ti_{0.05})(Ni_{0.85}Co_{0.15})_{3.5}$ hydrogen storage alloy was investigated systematically. The XRD results show that the main phases of the alloy are a $(LaMg)Ni_3$ phase with the $PuNi_3$-type rhombohedral structure and a $LaNi_5$ phase with the $CaCu_5$-type hexagonal structure. The electrochemical studies show that the maximum discharge capacity and the high rate dischargeability decrease with the increase of milling time. Furthermore, the exchange current density first increases and then decreases with the increase of milling time from 0 (as-cast) to 120 min, consistent with the variation of the charge-transfer resistance from the electrochemical impedance spectra. However, the limiting current density first decreases from 2472.8 mA/g (as-cast) to 1719.6 mA/g (BM 30 min) and then increases to 2360.4 mA/g (BM 120 min).

1 Introduction

Metal hydrides have been successfully used as the negative electrodes in nickel/metal-hydride (Ni/MH) secondary batteries due to their high-energy density, good charge and discharge ability, long cycling life and environmental compatibility.[1,2] Recently, several types of the hydrogen storage alloys have been extensively studied, including the rare earth-based AB_5-type alloys,[3] Ti-based or Zr-based AB_2-type alloys,[4] Mg-based alloys[5,6] and V-based solid solution alloys.[7] However, each type of alloy has its inherent advantages and disadvantages.[5-7] A few years ago, Kadir et al. reported a new series of ternary alloys with the formula of RMg_2Ni_9 (R = rare earth or Ca element), in which $(La_{0.65}Ca_{0.35})(Mg_{1.32}Ca_{0.68})Ni_9$ alloy could absorb 1.87 wt.% H_2 at 283 K under 0.01～3.30 MPa H_2 pressure.[8-11] Chen et al. investigated the structural and electrochemical characteristics of $LaCaMg(NiM)_9$ (M = Al, Mn) alloys, and obtained a maximum discharge capacity of 356 mAh/g.[12] Almost at the same time, the electrochemical properties and the crystal structures of La-Mg-$(NiCo)_x$ (x = 3–3.5) alloys were investigated by Kohno and coworkers.[13] Their results indicated that the maximum electrochemical discharge capacity of the $La_{0.7}Mg_{0.3}Ni_{2.8}Co_{0.5}$ alloy could reach a high value of 410 mAh/g and the cycling durability was quite good within 30 cycles. Liu et al. investigated the structural and electrochemical properties of $La_{0.7}Mg_{0.3}(Ni_{0.85}Co_{0.15})_{3.5}$, and a maximum discharge capacity of 396 mAh/g is achieved.[14-15] But the cycling life and the high rate dischargeability are too poor to be in practical application and therefore need to be improved. It is well known that, for hydrogen storage alloys, ball milling is a promising method for changing the morphology and crystal microstructure. For instance, Zaluski et al. reported that mechanical grinding is very effective for improving hydrogenation kinetics for Mg-based alloys.[16] Herein, in order to improve the overall properties of La-Mg-Ni-Co-type alloys, the effect of ball milling on the structure and electrochemical properties of $La_{0.7}(Mg_{0.25}Ti_{0.05})(Ni_{0.85}Co_{0.15})_{3.5}$ alloy was investigated systematically.

2 Experimental

$La_{0.7}(Mg_{0.25}Ti_{0.05})(Ni_{0.85}Co_{0.15})_{3.5}$ alloy was prepared by vacuum magnetic levitation melting under Ar atmosphere from component metals with the purity all above 99%.[17,18] Then, the ingot was mechanically crushed and ground into the powder of 200-mesh size. The alloy powder was ground by QM-1SP planetary ball mill under 0.1 MPa Ar for different times. In each stainless milling jar, the ball-to-powder weight ratio was set at 20:1. The structure of the alloys was characterized by XRD (Rigaku D/max-2500).

The details for the fabrication of the alloy electrode and the following electrochemical tests are described in our previous studies.[19] The charge-discharge cycle was conducted in a tri-electrode cell containing a counter electrode ($Ni(OH)_2$/NiOOH), a reference electrode (Hg/HgO), and a working electrode (the studied alloy) in an alkaline electrolyte (6 M KOH). The testing temperature was set at 30 °C.

3 Results and Discussion

3.1 Structure of $La_{0.7}(Mg_{0.25}Ti_{0.05})(Ni_{0.85}Co_{0.15})_{3.5}$ alloy

The XRD patterns of $La_{0.7}(Mg_{0.25}Ti_{0.05})(Ni_{0.85}Co_{0.15})_{3.5}$ alloy milled for different times are shown in Figure 1. It can be seen that as-cast and ball-milled alloys have a multiphase structure, in which the main phases consist of a $(LaMg)Ni_3$ phase with the $PuNi_3$-type rhombohedral structure and a $LaNi_5$ phase with the $CaCu_5$-type hexagonal structure. Figure 1 also shows that the diffraction peaks broaden with the increase of milling time, which indicates that the grain size decreases and the internal strain increases with proceeding milling. It is noted that a small diffraction peak of $(LaMg)Ni_3$ phase at

about 32° (2θ) appears for as-cast and ball-milled (30 min) alloys. However, this diffraction peak disappears with the increase of ball milling time to 60 min and 120 min, which indicates that the abundance of $(LaMg)Ni_3$ phase decreases due to its transformation into the $LaNi_5$ phase during ball milling.[20]

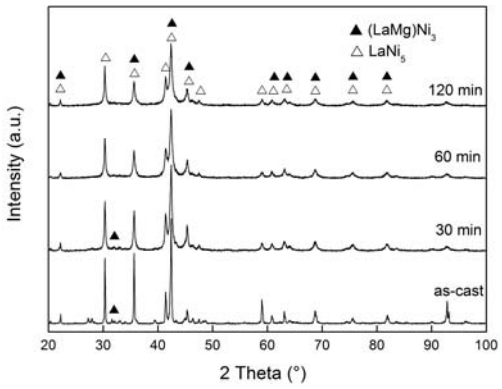

Figure 1. XRD patterns of $La_{0.7}(Mg_{0.25}Ti_{0.05})(Ni_{0.85}Co_{0.15})_{3.5}$ alloy milled for different times.

3.2 Discharge capacity and cycling life

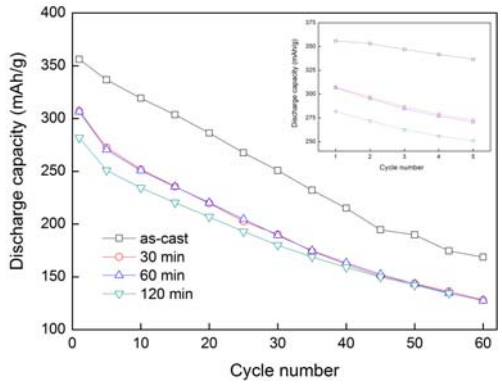

Figure 2. Cycling life of $La_{0.7}(Mg_{0.25}Ti_{0.05})(Ni_{0.85}Co_{0.15})_{3.5}$ alloy electrodes at 303 K milled for different times. The inset shows the activation.

The cycling life of $La_{0.7}(Mg_{0.25}Ti_{0.05})(Ni_{0.85}Co_{0.15})_{3.5}$ alloy electrodes milled for different times is shown in Figure 2. For as-cast and ball-milled alloys, the maximum capacity is achicved at the initial discharge cycle without any activation (see the inset in Figure 2), which would make them popular in practical applications. After ball milled for 120 min, the maximum discharge capacity decreases from 356.1 mA h/g for as-cast alloy to 281.7 mA h/g, which may be related to the decrease of the $(LaMg)Ni_3$ phase during milling process. Comparing the discharge capacity retention rate shown in Table 1, it can be found that the value of C_{60}/C_{max} after ball milling is slightly lower than that of as-cast alloy.

Table 1. Electrochemical properties of as-cast and ball-milled $La_{0.7}(Mg_{0.25}Ti_{0.05})(Ni_{0.85}Co_{0.15})_{3.5}$ alloy electrodes.

Samples	C_{max} (mAh/g)	N_a [a]	C_{60}/C_{max} (%)	HRD_{800} [b] (%)
As-cast	356.1	1	47.4	94.2
BM 30 min	307.2	1	41.7	93.8
BM 60 min	306.5	1	41.6	88.6
BM 120 min	281.7	1	45.4	91.8

[a] Cycle numbers needed to activate the alloy electrodes.
[b] High rate dischargeability at I_d = 800 mA/g.

3.3 Electrode reation kinetics

Figure 3 shows the relationship between the discharge capacity and the discharge current density of $La_{0.7}(Mg_{0.25}Ti_{0.05})(Ni_{0.85}Co_{0.15})_{3.5}$ alloy electrodes. The high rate dischargeability (HRD) is calculated according to the following formula: [21,22]

$$HRD = \frac{C_d}{C_d + C_{100}} \qquad (1)$$

It is found that both as-cast and ball-milled alloy electrodes have quite good HRD (see Table 1). In addition, the discharge capacity retention rate C_{60}/C_{max} and the HRD of the alloy electrodes first decrease and then increase with the increase of milling time. The minimum value of the discharge capacity retention rate C_{60}/C_{max} and the HRD is obtained when the alloy are milled for 60 min.

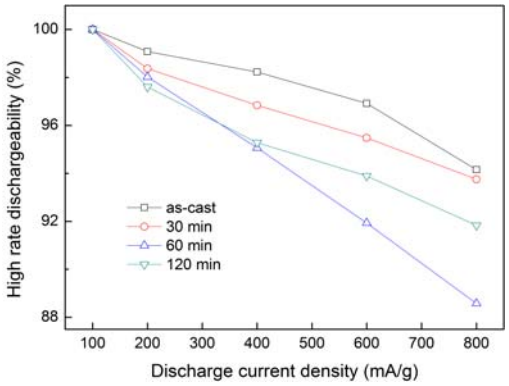

Figure 3. High rate dischargeability (HRD) of as-cast and ball-milled $La_{0.7}(Mg_{0.25}Ti_{0.05})(Ni_{0.85}Co_{0.15})_{3.5}$ alloy electrodes.

The electrochemical impedance spectra (EIS) of as-cast and ball-milled $La_{0.7}(Mg_{0.25}Ti_{0.05})(Ni_{0.85}Co_{0.15})_{3.5}$ alloy electrodes at 50% depth of discharge (DOD) are shown in Figure 4 (a). It can be seen that for all samples, each spectrum is composed of a smaller semicircle in the high-frequency region and a larger semicircle in the low-frequency region followed a straight line. Kuriyama et al. ascribed the measured high-frequency semicircle to the contact resistance between the current collector and the alloy pellet, the low-frequency semicircle to the reaction resistance, and the impedance between these two semicircles to the alloy particle-to-particle resistance. They attributed the observed low-frequency straight line to the Warburg impedance.[23] It is clearly seen that the contact impedance in the high-frequency region remains almost unchanged for the alloy electrodes with the

increase of milling time, but the radius of the larger semicircle in the low-frequency region decreases first with the increase of ball milling time and then increases. This variation indicates that the charge-transfer resistance of the alloy electrode decreases first to a minimum when the sample is ball-milled for 60 min and then increases to a higher value when the ball milling time is increased to120 min.

The exchange current density I_0 is a powerful parameter for measuring the kinetics of the electrochemical hydrogen reaction.[24,25] When the overpotential is changed within a small range, the exchange current density I_0 can be calculated by the following equation:[25]

$$I_0 = \frac{I_d RT}{F\eta} \qquad (2)$$

where R is the gas constant, T the absolute temperature, I_d the applied current density, F the faraday constant and η the total overpotential. Since RT/F is a constant for a given temperature, there is a linear relationship between the current density and the overpotential. Figure 5 (b) shows the linear polarization (LP) curves of as-cast and ball-milled $La_{0.7}(Mg_{0.25}Ti_{0.05})(Ni_{0.85}Co_{0.15})_{3.5}$ alloy electrodes. In all cases, a linear dependence is found in accordance with Eq. (2). The slope of the linear polarization curve corresponds to the polarization

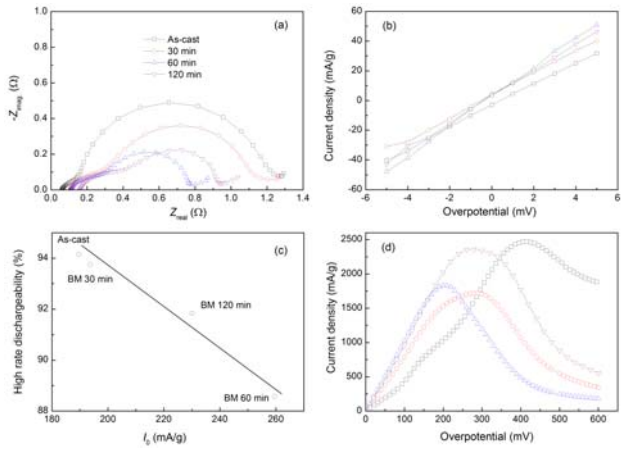

Figure 4. (a) Electrochemical impedance spectra (EIS), (b) Linear polarization curves, (c) Relationship between high high-rate dischargeability and exchange current density, and (d) Anodic polarization curves of as-cast and ball-milled $La_{0.7}(Mg_{0.25}Ti_{0.05})(Ni_{0.85}Co_{0.15})_{3.5}$ alloy electrodes at 50% DOD at 303 K.

Table 2. Polarization resistance R_p, Exchange current density I_0 and Limiting current density I_L of as-cast and ball-milled $La_{0.7}(Mg_{0.25}Ti_{0.05})(Ni_{0.85}Co_{0.15})_{3.5}$ alloy electrodes.

Samples	R_p (mΩ)	I_0 (mA/g)	I_L (mA/g)
As-cast	137.7	189.6	2472.8
BM 30 min	134.8	193.7	1719.6
BM 60 min	100.6	259.6	1832.2
BM 120 min	113.0	231.0	2360.4

resistance R_p of the alloy electrodes (see Table 2). R_p value first decreases from 137.7 mΩ (as-cast) to 100.6 mΩ (BM 60 min) then increases to 113.0 mΩ (BM 120 min). According to Eq. (2), I_0 values obtained for the various studied alloys are also listed in Table 2. With the increase of milling time from 0 (as-cast alloy) to 120 min, I_0 first increases from 189.6 mA/g to 259.6 mA/g and then decreases to 231.0 mA/g, which indicates that the kinetics of the electrochemical hydrogen reaction first increases and then decreases with the increase of the milling time. The variation is consistent with EIS results. This can be ascribed to an increase in the effective surface area during the milling. However, the reason why the kinetics of the electrochemical hydrogen reaction decreases when the milling time reaches 120 min may be related to the decrease in $(LaMg)Ni_3$ phase abundance.

Figure 4 (c) shows the relationship between HRD at 800 mA/g and the exchange current density of the as-cast and ball-milled $La_{0.7}(Mg_{0.25}Ti_{0.05})(Ni_{0.85}Co_{0.15})_{3.5}$ alloy electrodes. It can be seen that the HRD varies linearly with the exchange current density. It is generally accepted that the HRD is contorlled by the electrochemical kinetics on the surface and the hydrogen diffusion in the alloy. In case the electrochemical kinetics on the surface of alloy electrodes is the rate-determining factor, a linear dependence of the HRD on the exchange current density I_0 would be obtained. In contrast, if the diffusion rate hydrogen in the alloy is the rate-determining factor, the HRD would be a constant irrespective with the variation of the exchange current density I_0.[26] In this study, at 800 mA/g, HRD is essentially controlled by electrochemical reaction (charge-transfer reaction) on the surface of the alloy electrodes. However, with further increase in the discharge current density, the effect of hydrogen diffusion rate on HRD becomes more and more noticeable or the rate-determining step changes to a mixed control process of the charge-transfer reaction and the hydrogen diffusion in the bulk of the alloy.

Figure 4 (d) shows anodic polarization curves of as-cast and ball-milled $La_{0.7}(Mg_{0.25}Ti_{0.05})(Ni_{0.85}Co_{0.15})_{3.5}$ alloy electrodes. The limiting current density obtained (see Table 2) represents the hydrogen diffusion kinetics when hydrogen diffusion became the rate-determined step in the large overpotential region. I_L first decreases from 2472.8 mA/g (as-cast alloy) to 1719.6 mA/g (BM 30 min) and then increases to 2360.4 mA/g (BM 120 min). It can be believed that the larger the I_L value, the faster is the diffusion of the hydrogen atoms in the alloys.[24] The variation of the I_L values indicates that the hydrogen diffusivity in the alloy electrodes first decreases and then increases with the increase of the milling time.

4 Conclusions

In this paper, the effect of ball milling on the phase structure and the electrochemical properties of $La_{0.7}(Mg_{0.25}Ti_{0.05})(Ni_{0.85}Co_{0.15})_{3.5}$ hydrogen storage alloy was systematically studied. The results show that the alloy is consisted of a $(LaMg)Ni_3$ phase and a $LaNi_5$ phase. The maximum discharge capacity and HRD decrease with the increase of the milling time due to the decrease of the $(LaMg)Ni_3$ phase abundance. Moreover,

the charge-transfer resistance from EIS and the polarization resistance from anodic polarization first decrease (BM 60 min) and then increase (BM 120 min). The exchange current density corresponding to the polarization resistance increases from 189.6 mA/g (as-cast) to 259.6 mA/g (BM 60 min) and then decreases to 231.0 mA/g (BM 120 min), which indicates that the kinetics of the electrochemical hydrogen reaction have been improved after being ball-milled. The limiting current density first decreases from 2472.8 mA/g (as-cast alloy) to 1719.6 mA/g (BM 30 min) and then increases to 2360.4 mA/g (BM 120 min).

Acknowledgements

The authors wish to express their gratitude and appreciation for the financial support from the National Natural Science foundation of China (51361006, 51401059, 51461010, 51361005, 51371060, and 51461011), the Guangxi University Research Project (YB2014132) and the Guangxi Natural Science Foundation (2014GXNSFAA118043, 2013GXNSFBA019239, 2013GXNSFBA019034, 2014GXNSFAA118333).

References

[1] M. Tliha, C. Khaldi, S. Boussami, N. Fenineche, O. El-Kedim, H. Mathlouthi, J. Lamloumi, J. Solid State Electrochem. **18**, 577 (2014)
[2] Y.F. Liu, H.G. Pan, M.X. Gao, Q.D. Wang, J. Mater. Chem. **21**, 4743 (2011)
[3] Q.R. Yao, H.Y. Zhou, Z.M. Wang, S.K. Pan, G.H. Rao, J. Alloy Compd. **606**, 81 (2014)
[4] S.J. Qiu, J.L. Huang, H.L. Chu, Y.J. Zou, C.L. Xiang, H.Z. Zhang, F. Xu, L.X. Sun, H.Y. Zhou, J. Alloys Compd. **648**, 320 (2015)
[5] Y. Zhang, X.Y. Zhuang, Y.F. Zhu, L.Y. Zhan, Z.G. Pu, N. Wan, L.Q. Li, J. Alloys Compd. **622**, 580 (2015)
[6] Q.F. Tian, Y. Zhang, H.L. Chu, L.X. Sun, F. Xu, Z.C. Tan, H.T. Yuan, T. Zhang, J. Power Sources **159**, 155 (2006)
[7] M. Tsukahara, T. Kamiya, K. Takahashi, A. Kawabata, S. Sakurai, J. Shi, H.T. Takeshita, N. Kuriyama, T. Sakai, J. Electrochem. Soc. **147**, 2941 (2000)
[8] K. Kadir, T. Sakai, I. Uehara, J. Alloys Compd. **257**, 115 (1997)
[9] K. Kadir, N. Kuriyama, T. Sakai, I. Uehara, L. Eriksson, J. Alloys Compd. **284**, 145 (1999)
[10] K. Kadir, T. Sakai, I. Uehara, J. Alloys Compd. **287**, 264 (1999)
[11] K. Kadir, T. Sakai, I. Uehara, J. Alloys Compd. **302**, 112 (2000)
[12] J. Chen, N. Kuriyama, H.T. Takeshita, H. Tanaka, T. Sakai, M. Haruta, Electrochem. Solid-State Lett. **3**, 249 (2000)
[13] T. Kohno, H. Yoshida, F. Kawashima, T. Inaba, I. Sakai, M. Yamamoto, M. Kanda, J. Alloys Compd. **311**, L5 (2000)
[14] H.G. Pan, Y.F. Liu, M.X. Gao, Y.Q. Lei, Q.D. Wang, J. Electrochem. Soc. **150**, A565 (2003)
[15] Y.F. Liu, H.G. Pan, M.X. Gao, Y.F. Zhu, H.W. Ge, S.Q. Li, Y.Q. Lei, Acta Metall. Sin. **39**, 666 (2003)
[16] L. Zaluski, A. Zaluska, P. Ressier, J.O. StrÖm-Olsen, R. Schulz, J. Alloys Compd. **217**, 245 (1995)
[17] S.J. Qiu, J.L. Huang, H.L. Chu, Y.J. Zou, C.L. Xiang, H.Z. Zhang, F. Xu, L.X. Sun, L.Z. Ouyang, H.Y. Zhou, Metals **5**, 565 (2015)
[18] H.L. Chu, S.J. Qiu, Y. Zhang, L.X. Sun, F. Xu, M. Zhu, W.Y. Hu, Int. J. Hydrogen Energy **33**, 755 (2008)
[19] J.L. Huang, S.J. Qiu, H.L. Chu, Y.J. Zou, C.L. Xiang, H.Z. Zhang, F. Xu, L.X. Sun, L.Z. Ouyang, H.Y. Zhou, Int. J. Hydrogen Energy **40**, 14173 (2015)
[20] M. Zhu, C.H. Peng, L.Z. Ouyang, Y.Q. Tong, J. Alloys Compd. **426**, 316 (2006).
[21] H.L. Chu, Y. Zhang, S.J. Qiu, Y.N. Qi, L.X. Sun, F. Xu, Q. Wang, C. Dong, J. Alloys Compd. **457**, 90 (2008)
[22] S.J. Qiu, H.L. Chu, Y. Zhang, D.L. Sun, L.X. Sun, F. Xu, Int. J. Hydrogen Energy **34**, 7246 (2009)
[23] N. Kuriyama, T. Sakai, H. Miyamura, I. Uehara, H. Ishikawa, T. Iwasaki, J. Electrochem. Soc. **139**, L72 (1992)
[24] B.V. Ratnakumar, C. Witham, R.C. Bowman Jr., A. Hightower, B. Fultz, J. Electrochem. Soc. **143**, 2578 (1996)
[25] P.H.L. Notten, P. Hokkeling, J. Electrochem. Soc. **138**, 1877 (1991)
[26] C. Iwakura, T. Oura, H. Inoue, M. Matsuoka, Electrochim. Acta **41**, 117 (1996)